J. Fluid Mech. (1996), *vol.* 314, *pp.* 139–161

Two-dimensional vortex dynamics in a stratified barotropic fluid

By STEVE C. ARENDT

Laboratory for Atmospheric and Space Physics, University of Colorado, Boulder, CO 80309-0392, USA

(Received 18 July 1995 and in revised form 1 December 1995)

We show that two-dimensional 'point' vortex dynamics in both a polytropic fluid of $\gamma = 3/2$ and an isothermal fluid stratified by a constant gravitational field can be written in Hamiltonian form. We find that the formulation admits only one constant of the motion in addition to the Hamiltonian, so that two vortices are the most for which the motion is generally integrable. We study in detail the two-vortex problem and find a rich collection of behaviour: closed trajectories analogous to the circular orbits of the uniform-fluid two-vortex problem, open trajectories for which the self-propelled vortices scatter off each other, and both unstable and stable steadily translating pairs of vortices. Comparison is made to the case of two vortices in a uniform-density fluid bounded by a wall.

1. Introduction

Vortex dynamics in a constant-density fluid has a long history, beginning with the seminal work of Helmholtz (1867). For the case of a two-dimensional fluid, early work includes Helmholtz's treatment of the two-vortex problem, Kirchhoff's (1876) demonstration of the Hamiltonian nature of point vortex dynamics, and Grobli's solution (1877; see also Aref, Rott & Thomann 1992) of the three-vortex problem. More recently, interest has focused on, among other things, several-vortex systems (Novikov 1976; Novikov & Sedov 1978; Aref & Pomphrey 1982; Aref 1983), applications to two-dimensional turbulence (Onsager 1949; Kraichnan & Montgomery 1980; McWilliams 1990; Chorin 1994), and vortex dynamics in a rotating fluid (Morikawa 1960; Charney1963; Hogg & Stommel 1985), with the Hamiltonian formalism finding application in each.

Vortex dynamics in barotropic fluids stratified by a constant gravitational field has also been investigated (Arendt 1993*a*,*b*), but has received much less attention. Here the barotropic restriction prevents the usual baroclinic creation and destruction of vorticity so that Kelvin's theorem of conservation of circulation applies; vortices are persistent entities in such a fluid. The crucial effect of the density stratification is the self-propulsion of a straight vortex tube. This propulsion, which has no counterpart for vortex tubes in a uniform density fluid, is in the $\hat{\boldsymbol{g}} \times \hat{\boldsymbol{\omega}}$ direction, where $\hat{\boldsymbol{g}}$ is the direction of gravity, and has a magnitude roughly proportional to the inverse of the local density scale height of the fluid.

One expects the effect of stratification to be important when the density scale height of the fluid is comparable to other scales of a flow, e.g. the separation between vortices. The dependence of the self-propulsion on the inverse density scale height reflects this. Now, in the outermost regions of the convection zone of the Sun, the

density scale height becomes as small as 100 km, while fluid motion occurs on scales of 1000 km, taking granulation as an example. Here, then, the stratification and its consequent self-propulsion of vortices should be of prominent importance. Given the recent progress in using vortex dynamics to understand turbulence (Chorin 1994), we hope that the present results aid in understanding the dynamics of stratified-fluid turbulence as occurs in the convection zone of the Sun. Exploring this connection is left for future work, but it provides motivation for the present work.

Relaxing the barotropic assumption to allow for a stable stratification leads to baroclinic production of vorticity via the buoyancy force; such vorticity production is not contained in the analysis of the present paper. However, if the Froude number of the vortices is kept large, then the present results are still approximately valid. The Froude number is essentially the ratio of the buoyancy or Brunt–Väisälä timescale to the advective flow timescale. If the Froude number is much greater than one, then the buoyancy restoring force acts slowly and the flow is free to evolve (temporarily) advectively while weakly radiating internal gravity waves. On the other hand, if the Froude number is much less than one, then a vortex dissolves entirely into internal gravity waves on a timescale short compared to an advective timescale and the results of the present paper do not apply.

The purposes of the present paper are twofold: first, to develop the Hamiltonian formalism for two-dimensional point vortices in a barotropic stratified fluid, and second to provide a complete solution to the two-vortex problem. The latter is the simplest interaction described by the Hamiltonian, but it yields a startlingly rich array of vortex behaviour. We will also show that it is the only generally integrable interaction; the case of three or more vortices is non-integrable, at least in the absence of special symmetries. The analogous results for a uniform fluid are well known (Helmholtz 1867; Kirchhoff 1876; Aref 1983), and so a primary goal of this work is to investigate in detail the differences arising from the density stratification. It is here that the self-propulsion, primarily a density gradient effect, plays a crucial role.

Each particular density stratification unfortunately requires a separate, but similar, analysis. We investigate the particular cases of a polytropic fluid having $\gamma = 3/2$ and an isothermal fluid; the former is presented in the main text of the paper and the latter is contained in Appendix C. The general Hamiltonian formalism for the problem of N vortices appears in §2. In §3, we investigate the two-vortex problem in detail, dividing the problem into the case of like vortices (same sign of vorticity) and that of unlike vortices (different sign of vorticity). In §4, the results are summarized, and comparisons are made to uniform-density fluids, most notably a semi-infinite uniform-density fluid. Finally, Appendix A discusses the physical nature of the constants of the motion, and Appendix B reviews the two-vortex problem in a uniform fluid.

2. Hamiltonian formulation

In this section, we present a Hamiltonian formulation of two-dimensional vortex dynamics in a polytropic fluid layer stratified by gravity. We impose an impenetrable upper boundary on the fluid layer (such a boundary is generally necessary for barotropes to avoid an unphysical density, but see Appendix C for the case of an unbounded isothermal fluid), and denote the depth beneath this surface by $|z|$, letting z range from 0 to $-\infty$. The fluid is taken to have $\gamma = 3/2$ ($P = C\rho^{\gamma}$) to provide a rough match to solar conditions as well as for calculational convenience. The gravitational field is taken to be vertical and of constant magnitude, $\boldsymbol{g} = -g\hat{\boldsymbol{z}}$, so

that the hydrostatic density is $\rho = \rho_o(z/l)^2$, where ρ_o/l^2 is a known constant. Finally, the flow velocity is assumed slow compared to the local speed of sound, so that the pressure and density may be linearized about their hydrostatic values.

The simplest case of a single two-dimensional vortex has already been investigated extensively (Arendt 1993*a*,*b*), and we will use the results as the starting point for the present analysis. Consider, then, a vortex of strength $\kappa > 0$ (i.e. total circulation with positive being counterclockwise) located at $(y,z) = (y_o, z_o)$. Such a vortex is found to have a self-propulsion which propels it in the $-\hat{\boldsymbol{y}}$-direction, i.e. transverse to gravity. The self-propulsion is logarithmically singular in the ratio of the cross-sectional size to the density scale height, and so we cannot assume that the vortex is a true point vortex, but rather must endow it with a small, finite, cross-section. We will nonetheless continue to refer to these small vortices as 'point' vortices. Let the cross-section be circular (although strictly speaking there are small corrections added to this (Arendt 1993*b*)) with a radius given by b, and let b be small compared to the local density scale height given by $\lambda = (\mathrm{d}\ln\rho/\mathrm{d}z)^{-1} = z_o/2$.Within the circular core, the vorticity is taken to be proportional to the local density, so that the vorticity equation $\mathrm{D}(\omega/\rho)/\mathrm{D}t = 0$ is satisfied. Having these cross-sectional specifications, the vortex automatically adjusts its core to fit changes in local density, and does not undergo any additional core deformations. In this case, it has been shown (Arendt 1993*a*,*b*) that the streamfunction for the flow outside the vortex is

$$\psi = \frac{\kappa\rho_o}{2\pi l^2}\left[\frac{(y-y_o)^2 + z_o^2 + z^2}{4}\ln\left(\frac{(y-y_o)^2 + (z+z_o)^2}{(y-y_o)^2 + (z-z_o)^2}\right) - z_o z\right], \tag{2.1}$$

with the velocity field being given by $\rho\boldsymbol{u} = \hat{\boldsymbol{y}}\partial\psi/\partial z - \hat{\boldsymbol{z}}\partial\psi/\partial y$.

Using the fact that the vortex is transported by the local flow velocity, the equations of motion for the vortex are found to be (Arendt 1993*b*)

$$\frac{\mathrm{d}y_o}{\mathrm{d}t} = \frac{\kappa}{2\pi z_o}\left[\ln\left(\frac{2|z_o|}{b}\right) + \frac{1}{4}\right], \tag{2.2}$$

$$\frac{\mathrm{d}z_o}{\mathrm{d}t} = 0. \tag{2.3}$$

Equation (2.2) gives explicitly the self-propulsion of the vortex. Assuming a different cross-sectional shape will produce a slightly different mathematical form for the self-propulsion, but will not change the result in any essential way. This self-propulsion is mainly a result of the density stratification: the vortex is pushed horizontally by expanding rising fluid on one side and pulled by contracting sinking fluid on the other thereby giving a net horizontal migration which is singular as $b \to 0$ (see (2.2)). The presence of the upper boundary to the fluid layer also contributes to the self-propulsion somewhat, but its contribution does not depend on the core size of the vortex, and so it is not the dominant effect for small vortices. Furthermore, a vortex in an isothermal fluid without an upper boundary exhibits a similar self-propulsion (see Appendix C).

Next, consider the case of two vortices; the case of N vortices will be seen to be a straightforward extension. Let the two vortices have circulations κ_1 and κ_2, and be located at (y_1, z_1) and (y_2, z_2) respectively. Let both have cores as previously described with cross-sectional radii b_1 and b_2, each small compared to both the local density scale height and the distance between the two vortices; again, these specifications ensure that the vortex cores self-adjust to varying local changes in density and suffer no additional core deformations. The motion of the two vortices is the sum of their

self-motion and their mutually induced motion. The self-motion for each is of the form of (2.2)–(2.3), while the mutual interaction is found via the streamfunction given in (2.1). Adding these, the equations of motion for the vortices are found to be

$$\frac{dy_1}{dt} = \left(\frac{1}{\rho}\frac{\partial \psi_2}{\partial z}\right)_{y=y_1,\ z=z_1} + \frac{\kappa_1}{2\pi z_1}\left(\ln\left(\frac{2|z_1|}{b_1}\right) + \frac{1}{4}\right), \tag{2.4}$$

$$\frac{dz_1}{dt} = -\left(\frac{1}{\rho}\frac{\partial \psi_2}{\partial y}\right)_{y=y_1,\ z=z_1}, \tag{2.5}$$

$$\frac{dy_2}{dt} = \left(\frac{1}{\rho}\frac{\partial \psi_1}{\partial z}\right)_{y=y_2,\ z=z_2} + \frac{\kappa_2}{2\pi z_2}\left(\ln\left(\frac{2|z_2|}{b_2}\right) + \frac{1}{4}\right), \tag{2.6}$$

$$\frac{dz_2}{dt} = -\left(\frac{1}{\rho}\frac{\partial \psi_1}{\partial y}\right)_{y=y_2,\ z=z_2}, \tag{2.7}$$

where ψ_1 and ψ_2 are the streamfunctions of vortex 1 and 2 respectively, given by (2.1) with (y_o, z_o) replaced by (y_1, z_1) or (y_2, z_2).

Now, as a consequence of Kelvin's theorem and the continuity equation, the total circulation of each vortex and the total mass of the fluid inside of each vortex is conserved. The latter fact gives

$$(\pi b_i^2)\left(\frac{\rho_o z_i^2}{l^2}\right) = \text{constant}, \tag{2.8}$$

where $i = 1, 2$, and where the fact that each vortex is small compared to its local density scale height has been used. Equation (2.8) can be rewritten as

$$b_i = c_i/|z_i|, \tag{2.9}$$

where c_i is a constant. This is a physically reasonable result stating that the core size of the vortex decreases if the vortex moves into deeper, more dense, fluid.

Using (2.9), we rewrite (2.4)–(2.7) as

$$\frac{dy_i}{dt} = \frac{1}{3\kappa_i z_i^2}\frac{\partial H}{\partial z_i}, \tag{2.10}$$

$$\frac{dz_i}{dt} = -\frac{1}{3\kappa_i z_i^2}\frac{\partial H}{\partial y_i}, \tag{2.11}$$

where

$$H = \frac{3\kappa_1\kappa_2}{2\pi}\left[\frac{(y_1-y_2)^2 + z_1^2 + z_2^2}{4}\ln\left(\frac{(y_1-y_2)^2 + (z_1+z_2)^2}{(y_1-y_2)^2 + (z_1-z_2)^2}\right) - z_1 z_2\right] + \frac{3\kappa_1^2 z_1^2}{4\pi}\left[\ln\left(\frac{2z_1^2}{c_1}\right) - \frac{3}{4}\right] + \frac{3\kappa_2^2 z_2^2}{4\pi}\left[\ln\left(\frac{2z_2^2}{c_2}\right) - \frac{3}{4}\right]. \tag{2.12}$$

The first term in H is the mutual interaction found using (2.1),(2.5), and (2.7), while the last two terms are the self-interactions rewritten using (2.9) in (2.4) and (2.6). Defining the variables, $\eta_i = \kappa_i y_i$ and $\xi_i = z_i^3$, we arrive at the usual Hamiltonian form of equations (2.10) and (2.11):

$$\frac{d\eta_i}{dt} = \frac{\partial H}{\partial \xi_i}, \tag{2.13}$$

$$\frac{d\xi_i}{dt} = -\frac{\partial H}{\partial \eta_i}. \tag{2.14}$$

It is straightforward to show that for the general case of N vortices, the equations of motion are (2.13)–(2.14) with the Hamiltonian H given by

$$H = \sum_{i=1}^{N}\sum_{j=1}^{N} \frac{3\kappa_i\kappa_j}{4\pi}\left[\frac{(y_i-y_j)^2+z_i^2+z_j^2}{4}\ln\left(\frac{(y_i-y_j)^2+(z_i+z_j)^2}{(y_i-y_j)^2+(z_i-z_j)^2}\right)-z_iz_j\right]$$
$$+\sum_{i=1}^{n}\frac{3\kappa_i^2z_i^2}{4\pi}\left[\ln\left(\frac{2z_i^2}{c_i}\right)-\frac{3}{4}\right], \tag{2.15}$$

where $i \neq j$ in the double sum, and where an additional factor of $1/2$ has been added inside the double sum to avoid over-counting. Note that each vortex is characterized by a circulation strength κ_i as well as a cross-sectional size parameter c_i. Here again, we have assumed that the cross-sectional radii b_i, related to c_i through (2.9), are all small compared to both the local density scale heights $z_i/2$ and the distances to neighbouring vortices. It is a straightforward matter to show that if the density scale height is large compared to the separation between vortices, the above Hamiltonian reduces properly to that for a uniform-density fluid.

The Hamiltonian system (2.13), (2.14), and (2.15) admits two constants of the motion. The first is the Hamiltonian itself which may be shown to correspond to the total energy of the system (see Appendix A). In this regard, the first term on the right-hand side of (2.15) may be thought of as the interaction energy of the vortices, and the second term as the self-energies of the individual vortices.

The second constant of the motion is due to the invariance of the Hamiltonian with respect to translations in y_i, and is

$$Z^3 = \sum_{i=1}^{N}\kappa_i z_i^3 \Big/ \sum_{i=1}^{N}\kappa_i = \text{constant}. \tag{2.16}$$

The total circulation in the denominator of (2.16) cannot appear if it is zero; in this case, the expression (2.16) still applies with the term $\sum_{i=1}^{N}\kappa_i$ omitted. The quantity Z^3 is proportional to the total linear momentum in the $\hat{y}$-direction (see Appendix A). To verify that it is a constant of the motion, consider the Poisson bracket, defined as

$$[a,b] = \sum_{i=1}^{N}\left(\frac{\partial a}{\partial\xi}\frac{\partial b}{\partial\eta}-\frac{\partial a}{\partial\eta}\frac{\partial b}{\partial\xi}\right) = \sum_{i=1}^{N}\frac{1}{\kappa_i}\left(\frac{\partial a}{\partial z_i^3}\frac{\partial b}{\partial y_i}-\frac{\partial a}{\partial y_i}\frac{\partial b}{\partial z_i^3}\right). \tag{2.17}$$

The Poisson bracket between the Hamiltonian H and any constant of the motion must be zero. For simplicity, consider the particular case $N = 2$, for which we find

$$[Z^3,H] = \frac{\partial H}{\partial y_1}+\frac{\partial H}{\partial y_2} = \frac{\partial H}{\partial(y_1-y_2)}-\frac{\partial H}{\partial(y_1-y_2)} = 0, \tag{2.18}$$

where the intermediate step is valid because y_1 and y_2 appear only in the combination $(y_1 - y_2)$ in the Hamiltonian. The extension to the more general case of arbitrary N may be easily made.

We now proceed to show that (2.16) is the only invariant linear in the circulation strengths of the vortices, i.e. it is the only invariant of the form

$$F = \sum_{i=1}^{N}\kappa_i f(y_i,z_i^3). \tag{2.19}$$

First note that $f(y,z^3)$ must be independent of y. This follows from considering the

case of a single vortex, which, as previously explained, translates horizontally with a constant depth, z, and varying horizontal position, y. Any constant of the motion of the form (2.19), then, cannot depend on y. Next, taking the Poisson bracket of F with H for the special case of $N = 2$, we find

$$[F, H] = \frac{\mathrm{d}f(z_1^3)}{\mathrm{d}z_1^3}\frac{\partial H}{\partial y_1} + \frac{\mathrm{d}f(z_2^3)}{\mathrm{d}z_2^3}\frac{\partial H}{\partial y_2}. \tag{2.20}$$

Setting this equal to zero, we have

$$\frac{\mathrm{d}f(z_1^3)}{\mathrm{d}z_1^3} = \frac{\mathrm{d}f(z_2^3)}{\mathrm{d}z_2^3}, \tag{2.21}$$

where we have again used the fact that y_1 and y_2 appear only in the combination $(y_1 - y_2)$ in the Hamiltonian. Now, the left-hand side of (2.21) is a function of z_1 only and the right-hand side is a function of z_2 only; the only possible solution is

$$\frac{\mathrm{d}f(z^3)}{\mathrm{d}z^3} = C = \text{constant}. \tag{2.22}$$

Hence,

$$F = C\sum_{i=1}^{N} \kappa_i z_i^3, \tag{2.23}$$

so that F differs only by a constant of proportionality from Z^3 in (2.16). Thus Z^3 is the only linear invariant.

The fact that there are only two constants of the motion implies that $N = 2$ is the largest number of vortices for which the motion is generally integrable. This follows from the fact that an N-dimensional Hamilitonian system (i.e. $2N$ total coordinates and momenta) is integrable if it has N constants of the motion in involution, where the constants are in involution if the Poisson bracket of each constant with every other is zero (Whittaker 1959). This result implies that three vortices will be stochastic in some regions of phase space, whereas two vortices will be regular everywhere. We contrast this with the case of an unbounded uniform-density fluid for which there are three constants of the motion in involution so that $N = 3$ is the highest number for which the motion is integrable. Of course, the introduction of special symmetries may increase the number of vortices for which there is integrable motion.

It is of interest to ask where the effects of stratification appear in the Hamiltonian (2.15). Although the stratification affects the entire Hamiltonian to some degree, the principal effect lies in the self-energy (i.e. the second term in (2.15)), which is entirely absent from the Hamiltonian for an unbounded uniform-density fluid (see (B 1) in Appendix B). This term give rise to the self-propulsion of the vortices. A study of the two-vortex problem in the next section will reveal the changes that the presence of the self-energy introduces in the topology of the Hamiltonian contours. A similar self-energy is present for a bounded, semi-infinite uniform-density fluid (see (B 7) in Appendix B). Vortices for this case have a self-propulsion induced by the presence of the wall bounding the fluid. However, there is an important difference in these two self-propulsions in that the stratification self-propulsion depends on the cross-sectional size of the vortex (in this case through c_i), and can be made infinitely large by reducing the core size. On the other hand, the wall-induced self-propulsion depends only on the proximity of the vortex to the wall, and cannot be altered by changing the size of the vortex.

3. The two-vortex problem

In this section, we investigate the motion of a pair of vortices using the Hamiltonian derived in the previous section. The trajectories of the vortices are given by $H =$ constant from (2.12), subject to the constraint $Z^3 =$ constant in (2.16). The time behaviour of the vortices around these trajectories is obtained by a solution to the dynamical equations (2.13)–(2.14); we will not pursue the time behaviour in the present paper, but will concentrate only on the trajectories.

The description of the two-vortex problem is complicated by the presence of five parameters to be specified in (2.12) and (2.16): κ_1, κ_2, c_1, c_2, and Z^3. To simplify matters, we will assume that the cross-sectional size parameter, c_i, is identical for each vortex: $c_1 = c_2 = c$. Furthermore, we will normalize the position coordinates of the vortices by $|Z|$ in (2.16), using a tilde to denote normalized quantities,

$$\tilde{z}_1 = z_1/|Z|, \tag{3.1}$$

$$\tilde{z}_2 = z_2/|Z|, \tag{3.2}$$

$$\tilde{y} = (y_1 - y_2)/|Z|. \tag{3.3}$$

The normalized Hamiltonian is then

$$\tilde{H} = H\left(\frac{4\pi}{3\kappa_1^2 Z^2}\right) = \tilde{z}_1^2\left(\ln \tilde{z}_1^2 - 1 + \Gamma\right) + r^2\tilde{z}_2^2\left(\ln \tilde{z}_2^2 - 1 + \Gamma\right) + r\left(\frac{\tilde{y}^2 + \tilde{z}_1^2 + \tilde{z}_2^2}{2}\ln\left(\frac{\tilde{y}^2 + (\tilde{z}_1 + \tilde{z}_2)^2}{\tilde{y}^2 + (\tilde{z}_1 - \tilde{z}_2)^2}\right) - 2\tilde{z}_1\tilde{z}_2\right), \tag{3.4}$$

where we have defined $r = \kappa_2/\kappa_1$ and $\Gamma = \ln(2Z^2/c) + 0.25$. The normalized constant of the motion from (2.16) is

$$\tilde{z}_1^3 + r\tilde{z}_2^3 = \pm(1 + r), \tag{3.5}$$

where the sign on the right-hand side is chosen to be the sign of Z. Now there remain only two free parameters in (3.4) and (3.5): r, giving the relative strengths of the two vortices, and Γ, a measure of the cross-sectional size of the vortices. For convenience, we will restrict the range of r to $|r| > 1$; the range $0 < |r| < 1$ is available by switching the labels 1 and 2 on the vortices and is thus redundant.

The normalization (3.1)–(3.4) is not defined for the case $Z = 0$ which can occur for $r < 0$. In this case, we will simply omit the term Z from (3.1)–(3.4), as well as from the definition of Γ. The expressions (3.4) and (3.5) are retained, with the right-hand side of (3.5) being zero for this case.

3.1. *Vortex pair of like sign*

We begin with the case of like vortices ($r > 0$), i.e. vortices having circulations of the same sign. As mentioned, we restrict the range of r to $r \geqslant 1$. Before examining the topology of the trajectories, we note that equation (3.5) places strong restrictions on the relative locations of the vortices. Since $r \geqslant 1$ and $z_1, z_2 < 0$, the minus sign on the right-hand side of (3.5) applies. Equation (3.5) then implies that the two vortices are confined in a layer of fluid just under the surface and extending to a (normalized) depth of $-(1 + r)^{1/3}$ for $\tilde{z}_1$, and $-((1 + r)/r)^{1/3}$ for $\tilde{z}_2$. The vortices cannot travel past this depth, and, furthermore, if one vortex is at its maximum depth, the other must be simultaneously broaching the surface.

We solve (3.5) for $\tilde{z}_2$ as a function of $\tilde{z}_1$, and substitute this result into (3.4). The condition that the Hamiltonian is a constant of the motion then gives the vortex

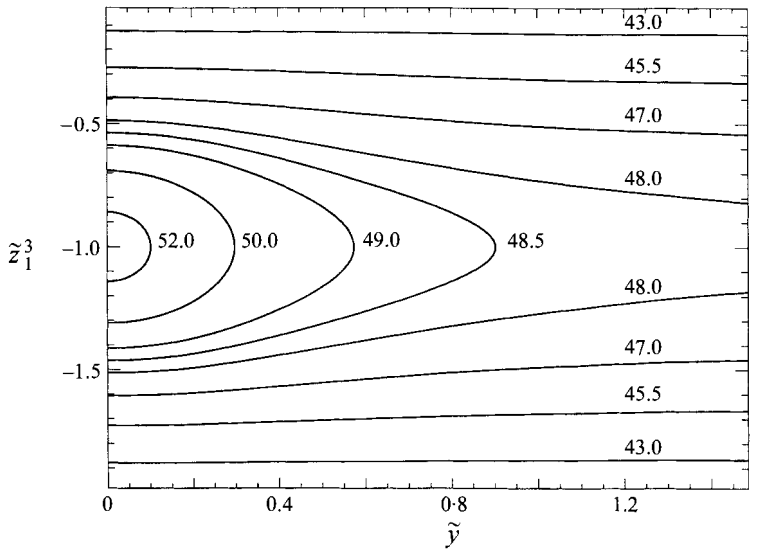

FIGURE 1. Contours of the Hamiltonian for $r = 1.0$ and $\Gamma = 25.0$ showing the central O-point.

trajectories in the plane $\tilde{z}_1^3$ versus $\tilde{y}$. As a first example, for $r = 1$ and $\Gamma = 25.0$ we obtain the contour map shown in figure 1. Since the Hamiltonian is symmetric in $\tilde{y}$, only half the domain is shown; the other half is obtained by reflecting about the $\tilde{z}_1^3$-axis. Figure 1 is plotted using the difference of the horizontal coordinates, $\tilde{y} = (y_1 - y_2)/Z$, so it represents the motion in a reference frame that moves along with the overall horizontal translation of the vortices; it displays the position of vortex #1 relative to the vertical upper boundary of the fluid layer and relative to the horizontal position of vortex #2. Of course, a similar figure can be made to show the position of vortex #2 instead.

Consider first the middle portion of figure 1. The O-point in the centre corresponds to the orbital O-point in the trajectories of the unbounded uniform-fluid two-vortex problem (see e.g. Appendix B). Close to the O-point the separation between the vortices is small compared to the local density scale height, so that the mutual interaction of the two dominates the self-propulsion and the vortices circle each other as they would in a uniform-density fluid. This O-point is present for any value of $r > 1$, and occurs at $\tilde{z}_1 = \tilde{z}_2$ for which $H \to -\infty$. Using (3.5), we find

$$(\tilde{z}_1)_{O\text{-}point} = (\tilde{z}_2)_{O\text{-}point} = -1, \tag{3.6}$$

$$(\tilde{y})_{O\text{-}point} = 0. \tag{3.7}$$

Of course, very close to the O-point, the 'point' vortex approximation breaks down, and the solution is no longer meaningful.

At a certain distance away from the central O-point, the orbits are no longer closed, but rather are open. In figure 1, the transition occurs at $\tilde{H} \simeq 48.0$. This is a consequence of the stratification, and, in particular, the self-propulsion of the individual vortices. If the vortices are sufficiently far apart, their self-propulsions are larger than the mutual interaction, which lessens with distance. One self-propulsion is generally larger than the other since each vortex has a different depth (see the functional dependence of the self-propulsion term in (2.2)), and so the vortices tend to separate, and eventually become infinitely far apart. The signature of the smaller

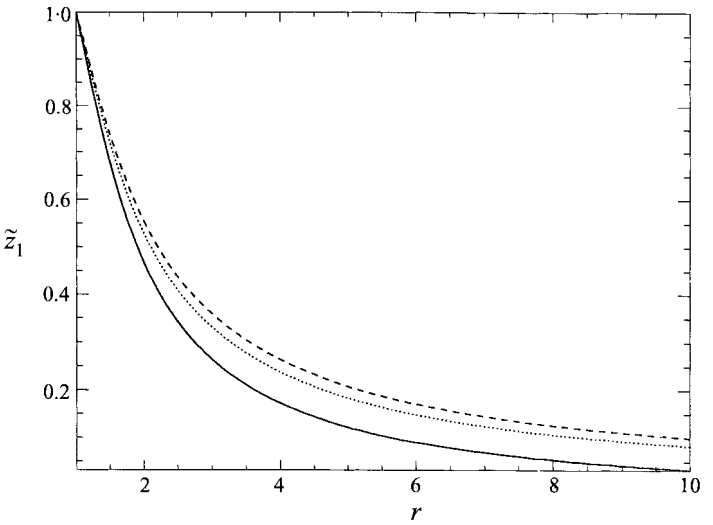

FIGURE 2. Location of the X-point at $\tilde{y} \to \infty$ for $r > 0$. The solid curve is for $\Gamma = 10.0$, the dotted curve, $\Gamma = 25.0$, and the dashed curve $\Gamma = 125.0$.

mutual effect can be seen in the open trajectories near $\tilde{y} = 0$ where each vortex is deflected from its otherwise straight path by its partner.

The sharpness of the transition between closed and open orbits in terms of the corresponding values of H is startling. The separatrix dividing the two sets may be thought of in terms of two X-points at $\tilde{y} \to \pm\infty$. The X-points are found by solving $\partial\tilde{H}/(\partial\tilde{z}_1^3) = 0$ as $\tilde{y} \to \pm\infty$. For a general value of $r > 1$, this gives the transcendental equation

$$\Gamma + \ln\tilde{z}_1^2 = \left(\frac{r\tilde{z}_1}{\tilde{z}_2}\right)\left[\Gamma + \ln\tilde{z}_2^2\right], \tag{3.8}$$

which may be solved numerically for each value of r and Γ; solutions are shown in figure 2.

If r is varied with Γ fixed, the symmetry about $\tilde{z}_1^3 = 1.0$ in figure 1 is lost, but the overall topology is unaffected until a critical value of r is reached. Above this critical value of r, a new pair of fixed points appears over the central O-point, as shown in figure 3 for the case $r = 2$ and $\Gamma = 25.0$. Here the new fixed points appear at $\tilde{z}_1^3 \simeq -0.35$ and $\tilde{z}_1^3 \simeq -0.63$. These fixed points have a finite value of the Hamiltonian (as opposed to the singular Hamiltonian for the central O-point), and correspond to steady translational solutions for the two vortices. That is, each fixed point represents the two vortices translating steadily as a pair, one above the other, with their self-propulsions and mutual interactions exactly balancing. Clearly, the O-point represents a stable translating pair and the X-point represents an unstable pair. The closed orbits in figure 3 now comprise three distinct sets: those surrounding the central O-point (e.g. $\tilde{H} = 131.5$), those surrounding the finite-$\tilde{H}$ O-point (e.g. $\tilde{H} = 130.35$), and those surrounding all three fixed points (e.g. $\tilde{H} = 129.9$). As before, open orbits reside at the very top and bottom of the domain.

To shed more light on these fixed points, we note that they may be determined by solving the equation $\partial H/\partial\tilde{z}_1 = 0$ along $\tilde{y} = 0$. The resulting transcendental equation

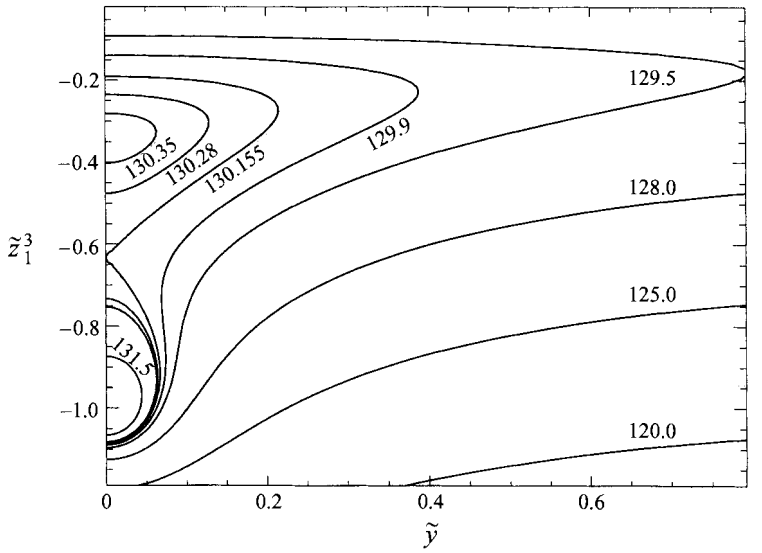

FIGURE 3. Contours of the Hamiltonian for $r = 2.0$ and $\Gamma = 25.0$ showing the central O-point and the X-O fixed point pair above it.

is found, after considerable algebra, to be

$$\Gamma = \ln\left[\frac{1+rx^3}{1+r}\right]^{2/3} + \frac{1-rx}{x-r}\ln\left|\frac{1+x}{1-x}\right| + \frac{1+rx}{x-r}\frac{2x}{1-x^2} + \frac{2r}{x-r}\ln x, \tag{3.9}$$

where we have defined x as

$$x = \frac{\tilde{z}_2}{\tilde{z}_1}, \tag{3.10}$$

and where we have used (3.5) in the simplification. Note that for a given choice of parameters Γ and r the left-hand side of (3.9) is a constant while the right-hand side varies only with the ratio x, with the applicable range for x being $0 < x < \infty$.

We will show in a moment that (3.9) has several solutions, but some of these will violate the 'point' vortex assumption that the core size of the vortices be small compared to both their local density scale heights and the distance between the two vortices. Mathematically, these conditions are

$$\frac{|\tilde{z}_1|}{\tilde{b}_1} = \frac{Z^2\tilde{z}_1^2}{c} > 10 \quad \rightarrow \quad \Gamma > \ln\left[20\left(\frac{1+rx^3}{1+r}\right)^{2/3}\right] + \frac{1}{4}, \tag{3.11}$$

$$\frac{|\tilde{z}_2|}{\tilde{b}_2} = \frac{Z^2\tilde{z}_2^2}{c} > 10 \quad \rightarrow \quad \Gamma > \ln\left[20\left(\frac{1+rx^3}{1+r}\right)^{2/3}\frac{1}{x^2}\right] + \frac{1}{4}, \tag{3.12}$$

$$\frac{|\tilde{z}_1 - \tilde{z}_2|}{\tilde{b}_1} = \frac{Z^2\tilde{z}_1|\tilde{z}_1 - \tilde{z}_2|}{c} > 10 \quad \rightarrow \quad \Gamma > \ln\left[20\left(\frac{1+rx^3}{1+r}\right)^{2/3}\frac{1}{|x-1|}\right] + \frac{1}{4}, \tag{3.13}$$

$$\frac{|\tilde{z}_1 - \tilde{z}_2|}{\tilde{b}_2} = \frac{Z^2\tilde{z}_2|\tilde{z}_1 - \tilde{z}_2|}{c} > 10 \quad \rightarrow \quad \Gamma > \ln\left[20\left(\frac{1+rx^3}{1+r}\right)^{2/3}\frac{1}{x|x-1|}\right] + \frac{1}{4}, \tag{3.14}$$

where we have put each condition into a form easily used in conjunction with (3.9).

Note that of the four conditions above, (3.12) is most stringent for $0 \leqslant x \leqslant 0.5$, (3.14) for $0.5 \leqslant x \leqslant 1.0$, (3.13) for $1.0 \leqslant x \leqslant 2.0$, and (3.11) for $2.0 \leqslant x \leqslant \infty$.

To proceed with an example of the solution of (3.9), the solid line in figure 4(*a*) shows the right-hand side of (3.9) as a function of x for $r = 2$. For a given value of Γ, a fixed point occurs where this function equals Γ. Also shown as a dotted line is the right-hand side of the condition that the 'point' vortex assumption not be violated, where we have taken the most stringent condition of the above four for each value of x. For a physical fixed point, the value of Γ chosen must lie above the dotted line at the location of the fixed point in x. From figure 4, we see that the pair of fixed points occurs for $\Gamma > 20.0$, and that the corresponding values of x for the fixed points lie between 1 and r. The overall shape of these curves (but not the details) persists as r is varied until $r > 7.57$, whereupon they change to those shown in figure 4(*b*) for the case $r = 8$. Here we see that fixed point solutions occur for roughly $\Gamma > 3.0$, and that one solution lies in the range $1 < x < r$ and the other in $x > r$. For lower values of Γ, fixed points will still occur in the topology of the orbits, but they will not be physical solutions for 'point' vortex motion.

3.2. *Vortex pair of unlike sign with* $Z \geqslant 0$

In this section we consider vortices having opposite signs. As explained previously, we will restrict our attention to the range $r \leqslant -1$; the range $-1 \leqslant r < 0$ may be explored by switching the labels on the two vortices, and so provides nothing new. As in the previous subsection, we will find that (3.5) restricts the relative positions of the two vortices strongly, and in fact determines to a great extent the topology of the trajectories. Given this, we subdivide the problem further into two parts: $Z \geqslant 0$ and $Z < 0$.

Consider the effect of equation (3.5) for the case $Z \geqslant 0$, for which we use the plus sign on the right-hand side of (3.5). Equation (3.5) implies that $|r|^{1/3}|\tilde{z}_2| \leqslant |\tilde{z}_1|$ so that $|\tilde{z}_1| \geqslant |\tilde{z}_2|$. Thus the stronger vortex (i.e. the vortex with the larger circulation) always lies shallower than the weaker vortex. We will have more to say about the implications of this in a moment.

In order to become familiar with an example, consider the case of two vortices having equal and opposite circulations, $r = -1$, and being symmetrically placed so that $Z = 0$. For this case the normalized expressions (3.1)–(3.5) are used with the term Z omitted. From (3.5), we find that $\tilde{z}_1 = \tilde{z}_2$, and the Hamiltonian becomes

$$\tilde{H} = 2\tilde{z}_1^2\left(\ln \tilde{z}_1^2 - 1 + \Gamma\right) - \left(\frac{\tilde{y}^2 + 2\tilde{z}_1^2}{2} \ln\left(\frac{\tilde{y}^2 + 4\tilde{z}_1^2}{\tilde{y}^2}\right) - 2\tilde{z}_1^2\right). \tag{3.15}$$

An example of the contours of constant H is shown in figure 5 for the case $\Gamma = 5.0$. As before, the Hamiltonian has reflection symmetry about the $\tilde{z}_1^3$-axis so that only the range $\tilde{y} > 0$ is shown. If the first vortex is placed on a given trajectory in figure 5, the second vortex occupies the same trajectory in the reflected portion of figure 5.

The vortices traverse the curves as a pair at an equal height, their direction of motion being determined by their relative signs. Suppose they traverse the curves from bottom to top. The mutual effect of one vortex on its partner is then to push it upward and attract it horizontally, while the self-propulsions, which in this case are in opposite directions, cause horizontal repulsion. The self-propulsions are here always stronger than the mutual attraction, and so the vortices move upward and apart. As they move upward, the local density scale height decreases so that their self-motions increase (see (2.2)) and they move apart at a faster rate. As they move apart, the mutual interaction decreases and their upward motion lessens. The vortex pair thus

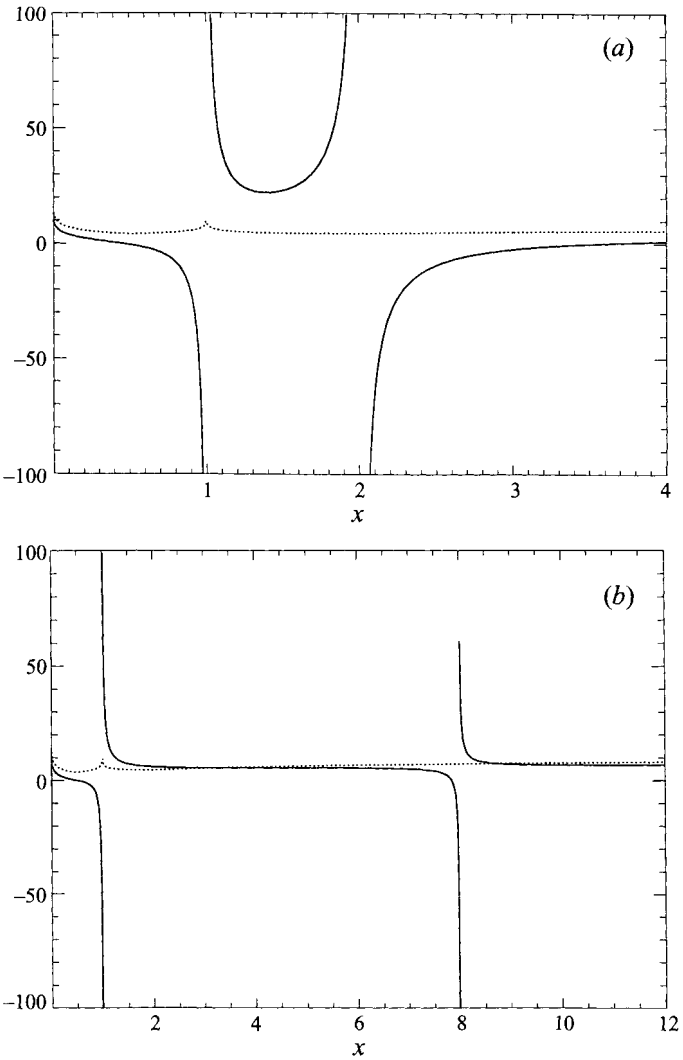

FIGURE 4. Right-hand side of (3.9) shown as a solid line and the most stringent of (3.11)–(3.14) shown as a dotted line, for (*a*) $r = 2.0$, (*b*) $r = 8.0$.

migrates upward at a steadily decreasing rate and spreads apart at an increasing rate, accounting for the transition from almost-vertical motion to almost-horizontal motion seen in figure 5.

Consider the asymptotic behaviour of the trajectories, beginning with $\tilde{y} \to \pm\infty$. In this limit, the mutual interaction term in the Hamiltonian goes to zero, and we find

$$\tilde{H} \to 2\tilde{z}_1^2 \left[\ln \tilde{z}_1^2 - 1 + \Gamma\right]. \tag{3.16}$$

The solution of this equation for a given value of $\tilde{H}$ gives the asymptotic vertical location of the vortices, as long as this solution satisfies the 'point' vortex condition that the cross-section be small compared to both the local density scale height, $z/2$, and the distance between the two vortices.

On the other hand, in the second asymptotic limit $\tilde{z}_1 \to -\infty$, it can be shown that the 'point vortex' approximation always breaks down. In this limit we have,

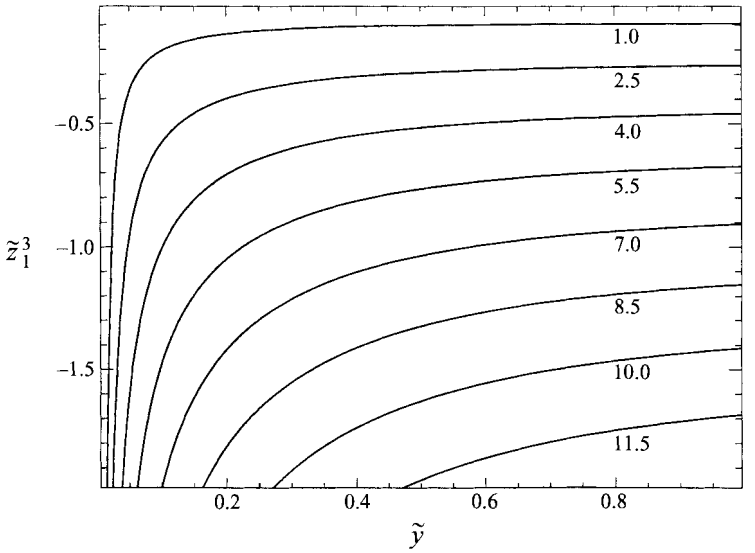

FIGURE 5. Contours of the Hamiltonian for $r = -1.0$, $\Gamma = 5.0$, and $Z = 0$, showing scattering trajectories.

from (3.15),

$$\tilde{H} \to 2\tilde{z}_1^2 \left[\ln \tilde{z}_1^2 + \Gamma - \tfrac{1}{2} \ln \left(\frac{4\tilde{z}_1^2}{\tilde{y}^2} \right) \right]. \tag{3.17}$$

As $\tilde{z}_1$ grows, the quantity inside the square brackets must decrease to maintain a finite value of $\tilde{H}$. In the limit where it decreases to zero we have

$$\frac{|\tilde{z}_1||\tilde{y}|}{2} = \mathrm{e}^{-\Gamma}. \tag{3.18}$$

Hence, $|\tilde{y}| \to 0$ as $\tilde{z}_1 \to -\infty$, but as this limit is attained we find

$$\frac{|\tilde{y}|}{\tilde{b}_1} = \frac{|\tilde{y}||\tilde{z}_1|Z^2}{c} = |\tilde{y}||\tilde{z}_1| \frac{\mathrm{e}^{\Gamma - 0.25}}{2} = \mathrm{e}^{-0.25} = 0.78, \tag{3.19}$$

which violates the point vortex approximation. Thus, at some depth the vortices always come close enough to interact strongly and cannot be treated as point vortices; they might be said to collide.

Next, retaining the zero on the right-hand side of (3.5), consider the more general case $r \neq -1$. As an example, curves of constant $\tilde{H}$ are shown in figure 6 for $r = -2$ and $\Gamma = 5.0$. Here the vortices may be thought of as scattering off each other. Suppose they start at $(y_1, z_1) = (+\infty, d_1)$ and $(y_2, z_2) = (-\infty, d_2)$, and begin moving inward due to their self-propulsions. The mutual interaction of each on the other pushes both downward, but due to their imbalance in strength the vortices do not move symmetrically ever downward as they did for $r = -1$. Rather, they pass each other, with the weaker going under the stronger. After passing, the mutual effects push each back upward, and they end their journey at $(y_1, z_1) = (-\infty, d_1)$ and $(y_2, z_2) = (+\infty, d_2)$. The case of $Z^3 > 0$ gives scattering-type trajectories similar to these, and yields nothing new.

It has probably not escaped the reader's attention that there are no fixed points in the trajectories of this subsection. This is entirely due to the stronger vortex lying always shallower than the weaker one, which was shown earlier. To see the connection

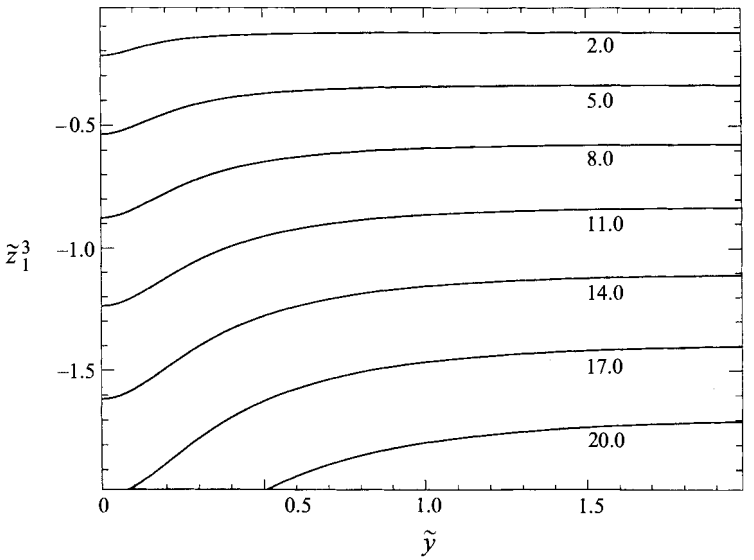

FIGURE 6. Contours of the Hamiltonian for $r = -2.0$, $\Gamma = 5.0$, and $Z = 0$, showing scattering trajectories.

to fixed points, first note that at a fixed point the Hamiltonian may be either singular or finite. A singular Hamiltonian corresponds to the two vortices orbiting around each other, as they do in the uniform-fluid two-vortex problem; clearly if one vortex is constrained to be below the other, as in the present case, they cannot orbit in this manner and so singular fixed points cannot occur.

The finite-Hamiltonian fixed point corresponds to a steadily translating pair of vortices. Now, for such a pair to exist, it has been shown (Arendt 1995) that it is necessary that $\hat{\boldsymbol{z}}\cdot(\boldsymbol{\kappa} \times \boldsymbol{U}_{translation}) > 0$. In the present case, this inequality is not satisfied. To see this, note that for $r < 0$ the lower vortex is propelled in the same direction by both its own self-propulsion and the mutual effect of the shallower vortex on it. It follows that the direction of translation of the pair as a whole must be in the direction of the self-propulsion of the lower vortex. This is such that $\hat{\boldsymbol{z}}\cdot(\boldsymbol{\kappa}_{lower} \times \boldsymbol{U}_{translation}) > 0$, and since the upper and lower vortices have opposite signs, $\hat{\boldsymbol{z}}\cdot(\boldsymbol{\kappa}_{upper} \times \boldsymbol{U}_{translation}) < 0$. Now, $|\kappa_{upper}| > |\kappa_{lower}|$ since the stronger vortex lies above than the weaker, and we have $\hat{\boldsymbol{z}}\cdot(\boldsymbol{\kappa}_{total} \times \boldsymbol{U}_{translation}) < 0$, which is the opposite of what is required. Therefore, steadily translating pairs of vortices, or, equivalently, finite-Hamiltonian fixed points, cannot occur for $Z > 0$.

3.3. *Vortex pair of unlike sign with $Z < 0$*

Consider next the case $Z < 0$, for which the minus sign on the right-hand side of (3.5) applies. For this case, equation (3.5) implies that $|r|^{1/3}|\tilde{z}_2| > |\tilde{z}_1|$ so that $|\tilde{z}_2/\tilde{z}_1| > |r|^{-1/3} < 1$; the stronger vortex can be either above or below the weaker vortex. We thus expect that fixed points will occur in the Hamiltonian contours.

A sample set of Hamiltonian contours for $r = -2.0$ and $\Gamma = 25.0$ is shown in figure 7(*a*). The enlargement of the region around $\tilde{z}_1 = -1.0$ in figure 7(*b*) shows two fixed points, the lower of which is the central O-point. Here, $\tilde{y} \to 0$ and $(\tilde{z}_1 - \tilde{z}_2) \to 0$ so that $\tilde{H} \to \infty$. From (3.5), the location of the O-point is given by (3.6) and (3.7) as before. Above the central O-point lies an X-point, at which the Hamiltonian is finite. The exact location of the X-point must be found numerically by searching for

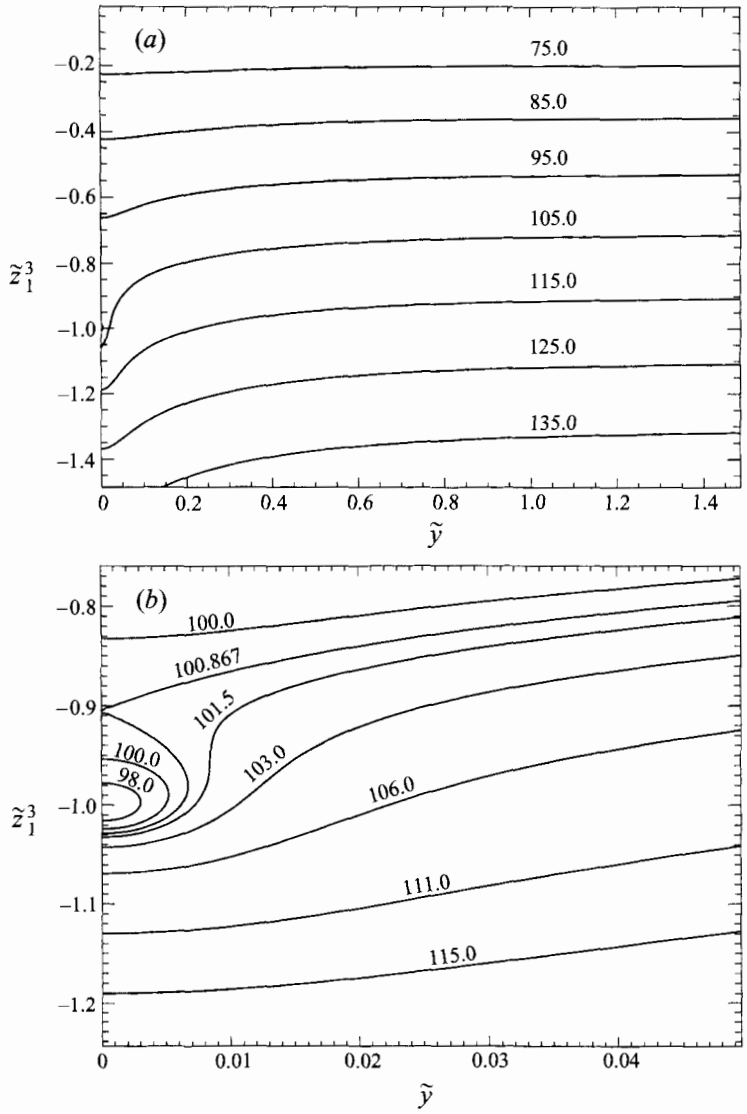

FIGURE 7. (*a*) Overview of contours of the Hamiltonian for $r = -2.0$, $\Gamma = 25.0$, and $Z < 0$, showing scattering trajectories. (*b*) Enlarged view showing the central O-point at $\tilde{z}_1^3 = -1.0$ with an X-point above.

a local minimum of the Hamiltonian along the $\tilde{z}_1^3$-axis. The governing equation has been given previously in (3.9), and the conditions for the fixed point to satisfy the 'point vortex' approximation are given in (3.11)–(3.14). An example of the right-hand side of (3.9) for $r = -2$ is shown in figure 8 as the solid curve with the condition for the point vortex approximation shown as the dotted curve. As before, the value of Γ at the location of the fixed point must be greater than the dotted curve. We see that there is one solution for a given Γ, as long as Γ is greater than about 3.0, and that it occurs at an x greater than 1.0. The overall shapes of the curves in figure 10 are unaffected by varying r; only the details change. We conclude that for a general $r < -1$, one X-point will be present in the topology of the orbits and that it will be physical as long as Γ is sufficiently large.

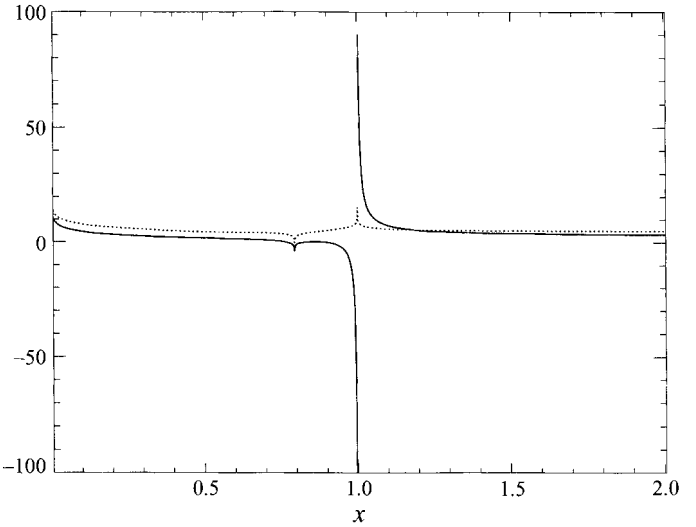

FIGURE 8. Right-hand side of (3.9) shown as a solid line and the most stringent of (3.11)–(3.14) shown as a dotted line, for $r = -2.0$.

Given the two fixed points, the orbits may be divided into a class of closed orbits as shown in figure 7(*b*), surrounded on all sides by open orbits as shown in both figures 7(*a*) and 7(*b*). The closed orbits are analogous to the closed circular orbits of two unlike vortices in a uniform fluid; as these are due to the mutual interaction, they only occur when the vortices are sufficiently close. The open orbits resemble those in figure 6, and have the same scattering interpretation. The X-point provides the separatrix between the sets of open and closed orbits. It represents a pair of vortices steadily propagating horizontally, one above the other, with self-propulsions and mutual effects exactly balancing. Note that the self-motions are in opposite directions, so that the vortices must be close enough to provide a strong mutual interaction capable of overriding the self-propulsions.

4. Discussion

In this paper we have demonstrated the Hamiltonian nature of the motion of small vortices in both polytropic and isothermal stratified fluids where each has been considered to be barotropic. We have derived the Hamiltonian and have shown that it corresponds to the total energy of the flow. We have also shown that there exists only a single additional constant of the motion; this corresponds to the horizontal linear momentum of the flow. It follows that two vortices are the most for which the motion is generally integrable in our fluid. For a higher number of vortices, the motion is non-integrable, at least in the absence of any special symmetries. For comparison, an unbounded uniform-density fluid has four constants of the motion (including the Hamiltonian) three of which are in involution, while a bounded semi-infinite uniform fluid has two constants of the motion, as in the present case. As a result, for an unbounded uniform fluid three vortices but no more exhibit integrable motion, while for a semi-infinite uniform fluid two vortices are the most for which the motion is integrable.

The lower number of constants of the motion for a stratified fluid has a further important effect for a set of like-signed vortices. In a uniform fluid, the constants of

the motion, in particular the angular momentum, serve to confine the vortices to a region surrounding a central point which is commonly called the *centre of vorticity*. However, in the stratified fluid case, we find that the vortices are only confined in the vertical direction (i.e. parallel to gravity), while their extent in the horizontal direction may be infinitely large. For example, an infinite separation occurs asymptotically in the open trajectories shown in figures 1 and 3. Physically, this result is due to the self-propulsion of the vortices: each vortex has its own motive power and can propel itself away from the others if their effects are not too great. A similar mechanism yields the same result for the semi-infinite uniform fluid, but vortices in an unbounded uniform fluid, having no self-propulsion, cannot separate themselves singly from the pack.

The second half of this paper investigates the case of two vortices in a polytropic fluid; these display a rich collection of solution trajectories, much more varied than the case of two vortices in an unbounded uniform fluid, but, as we shall see, very similar to those of a semi-infinite uniform fluid. To summarize the results of the paper, we find that the topology depends on the sign of the parameters r and Z and on the numerical value of Γ, where $r = \kappa_2/\kappa_1$ is a measure of the relative strength of the two vortices, Z is the conserved quantity corresponding to the linear momentum of the flow, and Γ, defined in §3, provides a measure of the cross-sectional size of the vortices. Focusing only on the fixed points of the Hamiltonian orbits, we find that for the case $r > 0$ there is always a central O-point at which the Hamiltonian is singular corresponding to mutually induced circular orbits of the two vortices, and there are two additional fixed points (one X-point and one O-point) if the value of Γ is sufficiently high. These last correspond to horizontally translating pairs of vortices; the X-point denotes an unstable pair, and the O-point a stable pair. For the case $r < 0$ and $Z < 0$, there is again a central O-point for which the two vortices orbit each other, and there is also an X-point if Γ is sufficiently large corresponding to an unstable translating pair of vortices. Finally, for the case $r < 0$ and $Z \geqslant 0$, there are no fixed points whatsoever.

It is interesting to compare these results to the case of a uniform-density fluid in order to determine the effect of the density stratification. For an unbounded uniform fluid, the Hamiltonian has an exceedingly simple topology: closed orbits surrounding a central O-point (at which the Hamiltonian is singular) for all cases except $r = -1$. For $r = -1$, the Hamiltonian contours are simply straight lines. As expected, the behaviour around the central O-point is reproduced for a stratified-fluid when the vortices are sufficiently close.

A better configuration for comparison is that of two vortices in a uniform-density fluid bounded above by a wall. For this case, the fluid possess an upper boundary like the polytropic fluid and the vortices have a self-propulsion similar to the stratified-fluid self-propulsion. This problem is reviewed in Appendix B. For the case of unlike vortices, $r < 0$, the Hamiltonian topology is the same as for the stratified fluid: if $Z < 0$, there is a central O-point at which the Hamiltonian is singular and an X-point at which the Hamiltonian is finite, while if $Z \geqslant 0$ there are no fixed points at all. However, for the case of like vortices, $r > 0$, differences arise. In particular, the semi-infinite uniform fluid contains only the central O-point, and not the two other fixed points found for the stratified fluid. Equivalently, steadily translating pairs of like vortices are not possible for a semi-infinite uniform fluid. Physically, this arises because the self-propulsion is not large enough to overcome the mutual interaction. This is not surprising, since this self-propulsion is due to the mutual effect of an image vortex, and so cannot be made large compared to the mutual interaction. On

the other hand, in a stratified fluid the self-propulsion is due primarily to the density stratification and is strongly dependent on the cross-sectional size of the vortex. As it can be made large compared to the mutual effects by making the vortex core smaller, we expect fixed points when Γ is large (which is the same as the cross-section being small), and this is precisely what we see. We conclude that the self-propulsion of vortices is the main effect of the density stratification, and that this is reflected in the topology of the Hamiltonian via both open trajectories and finite-Hamiltonian fixed points.

It is interesting to also look into the case of an isothermal fluid, which, unlike the polytropic fluid, requires no upper boundary. The Hamiltonian formulation is presented in Appendix C, and, although we do not do so here, one finds that the Hamiltonian topology for unlike vortices ($r < 0$) is the same as has been discussed above for the polytrope and the semi-infinite uniform fluid. However, for like vortices ($r > 0$) the central O-point is accompanied by two X-points, one above and one below. Thus, for different stratifications the presence of additional fixed points due to the self-propulsion seems to be robust, but their type and location is not.

We conclude by noting an unusual feature of the vortex self-propulsion, brought out by a comparison of the stratified fluid results with those for a uniform fluid. It seems reasonable to say that, in the case of two interacting vortices, stratification effects should become important when the density scale height of the fluid is comparable to, or smaller than, the separation between the vortices. This reasoning is true if the cross-sectional size of the vortices is not too small, since one can then show from (2.4) that the self-propulsion of the vortices is roughly $\kappa/(2\pi\lambda)$ where λ is the density scale height, and the mutual effect of each vortex on the other is of order $\kappa/(2\pi d)$ where d is the separation between the vortices. So if $\lambda \gg d$, the mutual effects are larger. However, if the core size, b, of the vortices is then made exceedingly small, the self-propulsion becomes infinitely large, being proportional to $\ln(b/\lambda)$, while the mutual interaction is unchanged if d is held fixed. Hence, the self-propulsion can be much larger than the mutual interaction even if $\lambda \gg d, b$. It is a unusual state of affairs wherein making the size of the vortex smaller compared to the density scale height *increases* the relative importance of the stratification-induced self-propulsion! The resolution of the paradox is found in noting that relative to a vortex's own local circulation, the size of the self-propulsion decreases as the cross-sectional size decreases, but relative to the (more or less fixed) mutual effect of neighbouring vortices, the self-propulsion increases. This effect is related to the set of fixed points for $r > 0$; these fixed points are dependent on a large self-propulsion for their existence and appear when the core size is sufficiently small.

Much of this work was completed at the High Altitude Observatory of the National Center for Atmospheric Research (NCAR); the author wishes to thank the Advanced Study Program for support while at NCAR. NCAR is sponsored by the National Science Foundation. Partial research support was also provided by the Norwegian Defence Research Establishment.

Appendix A

In this Appendix, we show that the Hamiltonian and the additional constant of the motion found in § 2 correspond to the fluid energy and linear momentum respectively. Consider first the energy of a collection of vortices. It has previously been shown (Arendt, 1993*c*) that the total energy (gravitational, internal, and kinetic) of a flow in

a barotropic stratified fluid with $v \ll c_s$ is equal to just the kinetic energy, and it may also be shown that the kinetic energy of such a flow in two dimensions is given by

$$E_k = \frac{1}{2}\int \psi\omega \, \mathrm{d}A, \tag{A 1}$$

where the area of integration is all space. If we denote the vorticity and streamfunction of the ith vortex by ψ_i and ω_i respectively, (A 1) becomes

$$E_k = \frac{1}{2}\sum_{i=1}^{n}\sum_{j=1}^{n}\int \psi_i\omega_j \, \mathrm{d}S. \tag{A 2}$$

The terms for which $i = j$ are the self-energy contributions which have previously been found to be (Arendt 1993*b*)

$$E_{self\ i} = \frac{1}{2}\int \psi_i\omega_i \mathrm{d}S = \frac{\kappa_i^2 z_i^2}{4\pi}\left(\frac{\rho_o}{l^2}\right)\left[\ln\left(\frac{2z_i}{b_i}\right) - \frac{3}{4}\right]. \tag{A 3}$$

The terms for which $i \neq j$ are the mutual interaction energies. Using the fact that the vortices are small in extent, these are found to be

$$E_{mutual\ ij} = \frac{1}{2}\int \psi_i\omega_j \mathrm{d}S \simeq \tfrac{1}{2}\kappa_j\psi_i(y_j, z_j)$$

$$= \frac{\kappa_i\kappa_j}{4\pi}\left(\frac{\rho_o}{l^2}\right)\left[\frac{(y_j - y_i)^2 + z_i^2 + z_j^2}{4}\ln\left(\frac{(y_j - y_i)^2 + (z_j + z_i)^2}{(y_j - y_i)^2 + (z_j - z_i)^2}\right) - z_i z_j\right]. \tag{A 4}$$

Using (A 3) and (A 4) in(A 2), we find the total kinetic energy

$$E_k = \sum_{i=1}^{n}\sum_{j=1}^{n}\frac{\kappa_i\kappa_j}{4\pi}\left(\frac{\rho_o}{l^2}\right)\left[\frac{(y_i - y_j)^2 + z_i^2 + z_j^2}{4}\ln\left(\frac{(y_i - y_j)^2 + (z_i + z_j)^2}{(y_i - y_j)^2 + (z_i - z_j)^2}\right) - z_i z_j\right]$$

$$+\sum_{i=1}^{n}\frac{\kappa_i^2 z_i^2}{4\pi}\left(\frac{\rho_o}{l^2}\right)\left[\ln\left(\frac{2z_i^2}{c_i}\right) - \frac{3}{4}\right]. \tag{A 5}$$

By comparing (2.15) and (A 5), we see that the Hamiltonian is proportional to the kinetic energy: $H = (3l^2/\rho_o)E_k$.

Consider next the total linear momentum of the flow. Because the integral of $\rho\boldsymbol{u}$ over all space is ill-defined in general (Batchelor 1967; Parker 1985), we will simply show that the linear momentum is proportional to $\sum \kappa_i z_i^3$ without determining the constant of proportionality. To do this, we first expand the streamfunction of a collection of vortices in the far field. Using $z = R\sin\theta$ and $y = R\cos\theta$ in (2.1), and letting $R \to \infty$, we obtain

$$\psi \simeq \frac{\rho_o}{2\pi l^2}\frac{4}{3}\frac{\sin^3\theta}{R}\sum_{i=1}^{N}\kappa_i z_i^3 + O(R^{-2}). \tag{A 6}$$

The linear momentum is then found from

$$\boldsymbol{P} = \int \rho\boldsymbol{u}\mathrm{d}A = \int \nabla\times\psi\hat{\boldsymbol{x}}\mathrm{d}A = -\int \psi\hat{\boldsymbol{x}}\times\mathbf{d}\boldsymbol{l}, \tag{A 7}$$

where the area of the integration is all space. Now, since $\psi \sim R^{-1}$ in the far field, we cannot substitute ψ directly into (A 7), as the integral over all space will not be well-defined. However, consider two flows each having the same value of $\sum \kappa_i z_i^3$. The

streamfunction for the difference between the two flows is then $\psi_{difference} \sim O(R^{-2})$. Using this in (A 7) and letting $R \to \infty$, we find that $\boldsymbol{P}_{difference} \sim O(R^{-1}) \to 0$. Thus, two flows having the same value of $\sum \kappa_i z_i^3$ have the same linear momentum, and we conclude that

$$\boldsymbol{P} \propto \hat{\boldsymbol{y}} \sum_{i=1}^{N} \kappa_i z_i^3. \tag{A 8}$$

This momentum is in the $\hat{\boldsymbol{y}}$-direction by virtue of the fact that the linear momentum in the $\hat{\boldsymbol{z}}$-direction must be identically zero. To prove this, note that the $\hat{\boldsymbol{z}}$-directed linear momentum is the integral of the $\hat{\boldsymbol{z}}$-directed mass flux. However, because of the impenetrable upper boundary on the fluid layer, the total mass flux across any horizontal plane is identically zero, and so the $\hat{\boldsymbol{z}}$-directed linear momentum is zero.

Appendix B

In this Appendix, we review the Hamiltonian formulation of two-dimensional uniform-fluid vortex dynamics, with emphasis on the two-vortex problem. To begin, it has long been known (Kirchhoff 1876; Aref 1983; Batchelor 1967) that the dynamics of two-dimensional point vortices in a uniform fluid admits the Hamiltonian

$$H = -\frac{1}{4\pi} \sum_i \sum_j \kappa_i \kappa_j \ln[(z_i - z_j)^2 + (y_i - y_j)^2], \tag{B 1}$$

where the double sum is not to include $i = j$, and the constants of the motion,

$$Z = \sum_i \kappa_i z_i \Big/ \sum_i \kappa_i, \tag{B 2}$$

$$Y = \sum_i \kappa_i y_i \Big/ \sum_i \kappa_i, \tag{B 3}$$

$$D^2 = \sum_i \kappa_i [(Z - z_i)^2 + (Y - y_i)^2] \Big/ \sum_i \kappa_i, \tag{B 4}$$

where we have assumed that $\sum_i \kappa_i \neq 0$. The constants of the motion H, Z, Y, and D^2 may be shown to correspond to the kinetic energy, the two components of the linear momentum, and the angular momentum respectively.

For the particular case of two vortices, equations (B 1)–(B 4) may be combined to yield

$$(z_1 - Z)^2 + (y_1 - Y)^2 = \left(\frac{\kappa_2}{\kappa_1 + \kappa_2}\right)^2 \exp\left[-\frac{4\pi H}{\kappa_1 \kappa_2}\right], \tag{B 5}$$

and

$$(z_2 - Z)^2 + (y_2 - Y)^2 = \left(\frac{\kappa_1}{\kappa_1 + \kappa_2}\right)^2 \exp\left[-\frac{4\pi H}{\kappa_1 \kappa_2}\right]. \tag{B 6}$$

Thus, the two vortices each follow circular paths about a common centre, but with different radii. This is true for all cases except for $\kappa_1 + \kappa_2 = 0$. In that case, the vortex pair propagates in a straight line and the separation between the two is unchanging. This might be considered a special case of the circular trajectory where the centre of the circle is removed to infinity and the radius becomes infinitely large.

The case of the stratified fluid bounded above studied in the present paper is

somewhat analogous to the case of a uniform-density fluid bounded by a wall. To permit a comparison, we briefly review the details of the two-vortex problem in such a fluid. Let two vortices with circulations κ_1 and κ_2 be located at (y_1, z_1) and (y_2, z_2) respectively (with $z_i < 0$), and suppose that a free-slip wall at $z = 0$ truncates the fluid layer. Using images to take account of the wall, the Hamiltonian is found from (B 1) to be

$$H = \frac{1}{4\pi}\left[\kappa_1^2 \ln(4z_1^2) + \kappa_2^2 \ln(4z_2^2) + 2\kappa_1\kappa_2 \ln\left(\frac{(z_1+z_2)^2+(y_1-y_2)^2}{(z_1-z_2)^2+(y_1-y_2)^2}\right)\right]. \tag{B 7}$$

The constant of the motion (B 2) is

$$Z = \frac{\kappa_1 z_1 + \kappa_2 z_2}{\kappa_1 + \kappa_2}, \tag{B 8}$$

while D^2 from (B 4) is proportional to Z, and Y given by (B 3) is identically zero.

To briefly describe the topology of the Hamiltonian, we determine the fixed points only. From the form of the Hamiltonian, it is clear that there is a singular point at $z_1 = z_2$ and $y_1 = y_2$. However, this singular point is not attained when $r < 0$ and $Z \geqslant 0$ for the same reasons as discussed in § 3 of the main body of the paper: the stronger vortex always lies above the weaker vortex.

For fixed points having a finite value of H, i.e. steadily translating pairs of vortices, we search for local extrema of the Hamiltonian along $y_1 - y_2 = 0$. Omitting the details, we find that $\partial H/\partial z_1 = 0$ if

$$x^3 + 3rx^2 + 3x + r = 0, \tag{B 9}$$

where $r = \kappa_2/\kappa_1$ and $x = z_2/z_1$. This cubic equation has only one real root; the root is greater than zero (as x has to be) when $r < 0$, and is given by

$$x_{fixed\ point} = [(r^2-1)(1-r)]^{1/3} - [(r^2-1)(1+r)]^{1/3} - r, \tag{B 10}$$

where each cubic root is chosen to be real. This fixed point can be shown to be an X-point, and is only attained when $Z < 0$.

We may summarize the topology of the trajectories as follows. For $r > 0$, there is one O-point at $x = z_2/z_1 = 1$ at which the Hamiltonian is singular. For $r < 0$ and $Z < 0$, there is again the O-point at $x = 1$, but there is also an X-point with a finite value of H at a location given by (B 10). For $r < 0$ and $Z \geqslant 0$, there are no fixed points at all.

Appendix C

In this Appendix, we present a Hamiltonian formulation for two-dimensional vortex dynamics in an isothermal stratified fluid whose hydrostatic density is given by $\rho = \rho_o \exp(-kz)$. The development follows that in § 2 for the polytropic stratified fluid. Here the self-propulsion of a circular vortex of radius b is given by (Arendt 1993*b*)

$$v_{self} = \frac{\kappa k}{4\pi}\left(\ln\left(\frac{bk}{2}\right) + \gamma - \frac{3}{4}\right)\hat{y}, \tag{C 1}$$

where $\gamma = 0.5772...$ is Euler's constant. The streamfunction outside a single vortex is given by

$$\psi_i = \frac{\kappa_i \rho_o}{2\pi} K_o\left[\frac{k}{2}((y-y_i)^2 + (z-z_i)^2)^{1/2}\right] \exp\left[-\frac{k}{2}(z+z_i)\right], \tag{C 2}$$

where K_o is the zeroth-order modified Bessel function of the second kind. It may then be shown that the Hamiltonian for an N vortex system is

$$H = -k\sum_{i=1}^{N}\sum_{j=1}^{N}\frac{\kappa_i\kappa_j}{4\pi}K_o\left[\frac{k}{2}((y_i-y_j)^2+(z_i-z_j)^2)^{1/2}\right]\exp\left[-\frac{k}{2}(z_i+z_j)\right]$$
$$+k\sum_{i=1}^{N}\frac{\kappa_i^2}{4\pi}\left[\ln\left(\frac{kc_i}{2}\right)+\gamma-\frac{1}{4}+\frac{kz_i}{2}\right]\exp[-kz_i], \tag{C 3}$$

where c_i is found from the conservation of mass within the vortex:

$$b_i = c_i\exp\left[\frac{kz_i}{2}\right]. \tag{C 4}$$

The Hamiltonian equations of motion are given by (2.13) and (2.14) with $\eta_i = \kappa_i y_i$ and $\xi_i = \exp(-kz_i)$. As in the polytropic case, only one constant of the motion in addition to the Hamiltonian exists; it is given by

$$\exp(-kZ) = \sum_{i=1}^{N}\kappa_i\exp(-kz_i)\Big/\sum_{i=1}^{N}\kappa_i. \tag{C 5}$$

The trajectory topology for the two-vortex problem using this Hamiltonian is briefly addressed in § 4.

REFERENCES

AREF, H. 1983 Integrable, chaotic, and turbulent vortex motion in two-dimensional flows. *Ann. Rev. Fluid Mech.* **15**, 345–389.

AREF, H. & POMPHREY, N. 1982 Integrable and chaotic motions of four vortices I. the case of identical vortices. *Proc. R. Soc. Lond.* A **380**, 359–387.

AREF, H., ROTT, N. & THOMANN, H. 1992 Grobli's solution of the three-vortex problem. *Ann. Rev. Fluid Mech.* **24**, 1–20.

ARENDT, S. 1993*a* Vorticity in stratified fluids I: general formulation. *Geophys. Astrophys. Fluid Dyn.* **68**, 59–83.

ARENDT, S. 1993*b* Vorticity in stratified fluids II: finite cross-section filaments and rings. *Geophys. Astrophys. Fluid Dyn.* **70**, 161–193.

ARENDT, S. 1993*c* On the dynamical buoyancy of vortices. *Astrophys. J.* **412**, 664–674.

ARENDT, S. 1995 Steadily translating vortices in a stratified fluid. *Phys. Fluids* **7**, 384–388.

BATCHELOR, G. K. 1967 *An Introduction to Fluid Dynamics.* Cambridge University Press.

CHARNEY, J. G. 1963 Numerical experiments in atmospheric hydrodynamics. In *Proc. Symp. Appl. Math. Am. Math. Soc.* **15**, 289–310.

CHORIN, A. J. 1994 *Vorticity and Turbulence.* Springer.

GROBLI, W. 1877 *Specielle Probleme uber die Bewegung Geradliniger Paralleler Wirbelfaden.* Zuricher und Furrer.

HELMHOLTZ, H. 1867 On the integrals of the hydrodynamical equations which express vortex-motion (transl. by P. G. Tait). *Phil. Mag.* (4) **33**, 483–512.

HOGG, N. G. & STOMMEL, H. M. 1985 The heton, an elementary interaction between discrete baroclinic geostrophic vortices, and its implications concerning eddy heat-flow. *Proc. R. Soc. Lond.* A **397**, 1–20.

KIRCHHOFF, G. R. 1876 *Vorlesungen uber Matematische Physik.* Teubner.

KRAICHNAN, R. B. & MONTGOMERY, D. 1980 Two dimensional turbulence. *Rep. Prog. Phys.* **43**, 547–619.

MCWILLIAMS, J. C. 1990 The vortices of two-dimensional turbulence. *J. Fluid Mech.* **219**, 361–385.

MORIKAWA, G. K. 1960 Geostrophic vortex motion. *J. Met.* **17**, 148–158.

NOVIKOV, E. A. 1976 Dynamics and statistics of a system of vortices. *Sov. Phys.-JETP* **41**, 937–943.

NOVIKOV, E. A. & SEDOV, YU. B. 1978 Vortex collapse. *Sov. Phys.-JETP* **50**, 297–301.

ONSAGER, L. 1949 Statistical hydrodynamics. *Nuovo Cimento Supp.* **6**, 279–287.

PARKER, E. N. 1985 Stellar fibril magnetic systems II: two-dimensional magnetohydrodynamic equations. *Astrophys. J.* **294**, 47–56.

WHITTAKER, E. T. 1959 *A Treatise on the Analytical Dynamics of Particles and Rigid Bodies.* Cambridge University Press.